Journal of Achievements in Materials and Manufacturing Engineering
VOLUME 19
ISSUE 1
November
2006

Acoustic emission in drilling carbon steel and nodular gray iron

J. Kopač*, S. Sali
Faculty of Mechanical Engineering, University of Ljubljana,
Askerceva 6, 1000 Ljubljana, Slovenia
* Corresponding author: E-mail address: janez.kopac@fs.uni-lj.si

Received in revised form 15.07.2006; accepted 30.09.2006

Manufacturing and processing

ABSTRACT

Purpose: of this paper is to investigate tool wear monitoring of drilling process by acoustic emission (AE).
Design/methodology/approach: of tool wear monitoring in drilling acquires the AE signal and analyses it in the frequency domain.
Findings: Tool wear in drilling significantly influences the AE signal independently of the measuring method. This influence is evidently different for various materials. The distance between the sensor and borehole has no significant effect on AE signal.
Research limitations/implications: A low S/N ratio and sensors with variable frequency response are undesirable characteristics of AE measurements. The significant correlations between the AE signal and characteristics of the cutting process are valid only within certain limits of cutting parameters.
Practical implications: The proposed measurements arrangement enables the development of an online drilling tool wear monitoring system, which can be used in serial production.
Originality/value: The paper evaluates drill wear effect on AE energy spectra for different workpiece materials
Keywords: Drilling; Acoustic emission; Monitoring; Tool wear

1. Introduction

The demands on manufacturing technology to improve the productivity by reducing production time have significantly increased during the last years. The demands can be complied with successful monitoring [1,2,3] and reduction of tool wear [4,5,6,7]. In this paper, AE sensing [8,9,10,11] was employed for online drilling monitoring in terms of a tool wear.

As shown in Figure 1, the paper discusses the drilling into two different materials (C15E steel, GG40 nodular gray iron) and the corresponding analysis of AE signal in frequency domain. Other variables investigated were (i) the distance between the sensor and borehole, and (ii) drill wear.

2. Experimental work

2.1. Definitions

The workpieces and measurement arrangement are shown in Figure 2 and Figure 3, respectively. The rotational speed of the drill was 400 rev/min and the feed rate was 0.08 mm/rev. The input into the digital oscilloscope was voltage from the amplifier. This voltage represents a function dependent on time and it was transformed into the frequency domain before the analysis. The discrete amplitude spectrum $S'(m{\cdot}\Delta f)$ of the recorded AE signal was calculated with the Fast Fourier Transform (FFT) technique [12]:

$$S'(m\cdot\Delta f)=\frac{T}{N}\sum_{n=0}^{N-1} f(n\cdot\Delta t)\cdot \mathrm{e}^{-\mathrm{j}2\pi mn/N} \tag{1}$$

where m = 1, 2 ... N/2, Δf is frequency lines spacing, T time of recording, N number of samples, Δt time interval between samples, $f(n\cdot\Delta t)$ a digital value of a record at point n and j is $\sqrt{-1}$. The one-sided amplitude spectrum $S(m\cdot\Delta f)$ in units of Volt is defined as [13]:

$$S(m\cdot\Delta f)=2\frac{|S'(m\cdot\Delta f)|}{N} \tag{2}$$

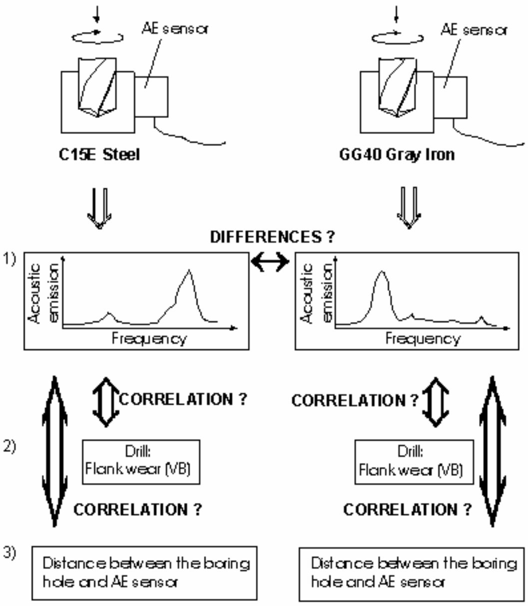

Fig. 1. Concept of experimentation

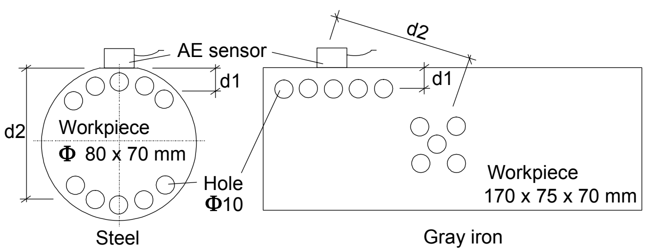

Fig. 2. The workpieces and distances between the sensor and borehole - d1, d2

In each of 5 holes (depth ≈ 30 mm) 60 recordings of AE signal were made, which resulted in 300 (5×60) amplitude spectra $S(m\cdot\Delta f)$. Out of these 300 single spectra the average spectrum was calculated:

$$\overline{S(m\cdot\Delta f)}=\frac{1}{300}\sum_{i=1}^{300} S_i(m\cdot\Delta f) \tag{3}$$

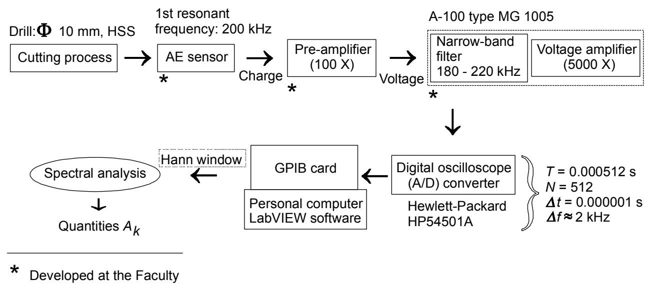

Fig. 3. Measurement arrangement

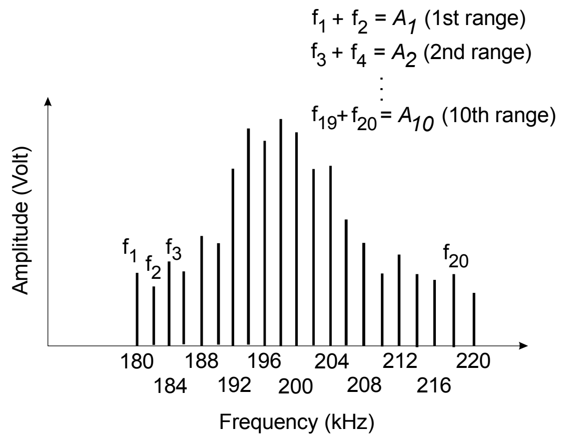

Fig. 4. Ranges of one-sided average amplitude spectrum of filtered AE signal (f_i; frequency line, i = 1 … 20)

Before the digitalization the Hann windowing of each AE signal was performed.

The analyzed range of the average spectrum from 180 - 220 kHz was divided into ten almost 4 kHz wide frequency ranges k (k=1 … 10) as shown in Figure 4. Thus, each frequency range consists of two neighboring frequency lines. The sum of the k-th pair of frequency lines represents the amplitude A_k of the k-th frequency range of the average spectrum in Volt units (k=1 to 10).

2.2. The influence of the distance between the borehole and sensor

Figure 5 shows the influence of the distance (see Figure 2) between the sensor and borehole for both materials. In these measurements, the flank wear of the drill (VB) was approximately 0.02 mm. For steel and for gray iron the distances d1 and d2 had no significant effect on A_k 's. The comparison of two A_k 's (k = const.) corresponding to distances d1 and d2 was performed by t- and F-tests at a level of confidence 5%. For both distances d1 and d2, the amplitudes were significantly higher for all ranges, when drilling into steel.

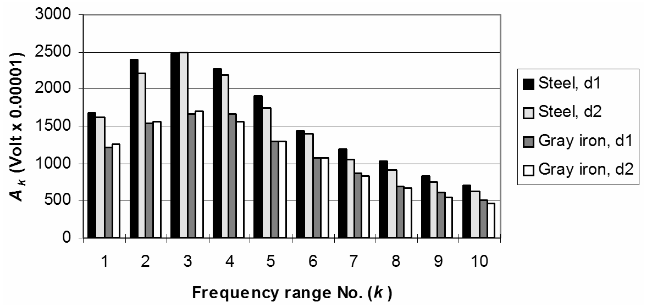

Fig. 5. The influence of the distance between the sensor and borehole

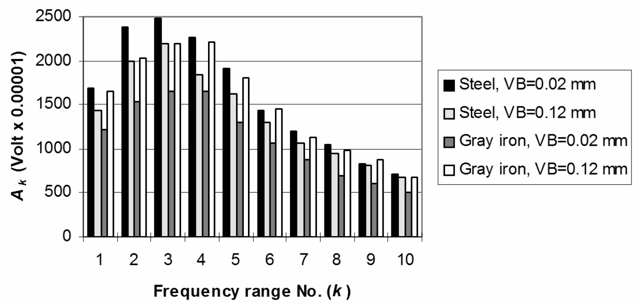

Fig. 6. The influence of flank wear on AE signal

2.3. The influence of flank wear on AE signal

Figure 6 shows the influence of the drill wear for both materials. In these measurements the distance between the sensor and borehole was d1. The comparison of two A_k 's ($k = \text{const.}$) was performed in the same way as described above. Drilling into steel at VB = 0.12 mm resulted in lower amplitudes than at VB = 0.02 mm, but only for the 4th frequency range a significantly lower amplitude was calculated. In contrast, drilling into gray iron at VB = 0.12 mm resulted in amplitudes significantly higher than at VB = 0.02 mm in all frequency ranges.

Next, for VB = 0.12 mm, drilling into steel compared to drilling into gray iron did not result in significantly different amplitudes in any frequency range. In addition, drilling into steel at VB = 0.02 mm did not result in significantly different amplitudes when compared to drilling into gray iron at VB = 0.12 mm in any frequency range.

3. Discussion

It is evident from Figure 5 that a significantly lower energy of AE at VB=0.02 mm was detected for gray iron in comparison to steel, irrespective of the distance between the sensor and borehole. This could be explained with graphite nodules in gray iron. As evident from Figure 7, a relatively high portion of carbon (black) in gray iron in comparison to steel could be a reason for relatively high losses of AE signal and higher damping, respectively. The increase in distance from d1 to d2 resulted in an insignificant decrease in the energy of AE. This is also logical because a larger distance means larger dissipation of AE waves, propagating within the workpiece. The energy in drilling into steel at VB=0.02 mm was significantly higher in only one frequency range in comparison to the situation when VB was 0.12 mm. In drilling into gray iron the tool wear had a significant influence for all frequency ranges, therefore we can say that the flank wear significantly influenced the AE signal in both materials. At VB=0.02 mm the energy of AE signal was significantly higher when drilling into steel but at VB=0.12 mm it was statistically equal for both materials. Briefly, the influence of tool wear showed a different but significant effect on AE signal for both tested materials. In addition, the assumed relatively high losses of the AE signal due to graphite nodules in gray iron are not a satisfactory explanation of the measured data. Namely, the statistical equality of the energy of the AE signal for both materials at VB=0.12 mm was calculated. This indicates a higher complexity of AE signal formation in and near the cutting zone: Most probably the reasons for the measured data are (i) chip breakage and impacts of the chip into the workpiece and (ii) friction between the tool and chip on the rake face, and between the worn-down clearance face and workpiece which is shownin Figure 8.

One can see that monitoring of tool wear over the frequency spectrum of the AE signal is actually possible. However, it may reasonably be supposed that a physical explanation of the measured results would be too complex and will not be considered here. In order to learn more about the influence of the tool wear and some other parameters on the AE signal, an additional experiment with the fluidic AE sensor was performed.

The most appropriate place for tool wear monitoring by an AE sensor is the tool itself. The jet of coolant fluid was directed into the drill as indicated in Figure 9 where also the workpiece, tool, shield (protection against chips), and reservoir for coolant (emulsion) are shown. In these experiments only drilling in C15E steel was performed. Measurement arrangement, signal processing and the shape of the workpiece were the same as in experiments with a contact AE sensor (see Figures 2, 3 and 4). In these measurements the mean value of the 10 quantities A_k (see Figure 4) corresponding to each frequency spectrum (see equation (2)) was calculated:

$$A = \frac{1}{10}\sum_{k=1}^{10} A_k \tag{4}$$

Next, the mean value of the 300 single A's was calculated which resulted in the mean amplitude of the average spectrum:

$$\overline{A} = \frac{1}{300}\sum_{1}^{300} A \tag{5}$$

The following measurements where the cutting parameters were variables were performed:

a) Cutting conditions:
- rotational speed: 400 rev./min,
- feed rate: 0.08 mm/rev.,
- flank wear VB = 0 mm (+0.03 mm).

b) Cutting conditions:
- rotational speed: 560 rev./min,
- feed rate: 0.08 mm/rev.,
- flank wear VB = 0 mm (+0.03 mm).

c) Cutting conditions:
- rotational speed: 400 rev./min,
- feed rate: 0.12 mm/rev.,
- flank wear VB = 0 mm (+0.03 mm).

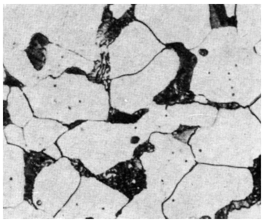

Carbon: 0.15 - 0.18%

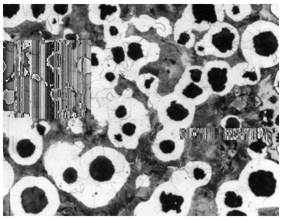

Carbon: ca. 3%

Fig. 7. Microstructure of the tested materials: (a) C15E, ca. 1:350; (b) GG40, ca. 1:40

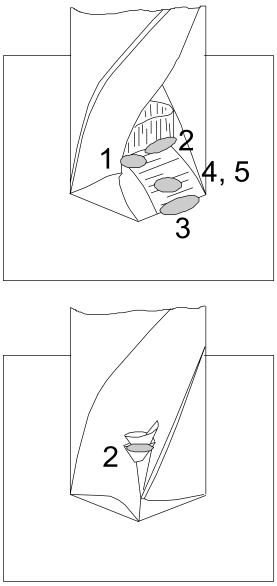

- chip breakage and impacts of the chip into the workpiece (1, 2)

- friction between tool and chip on the rake face, and between the worn-down clearence face and workpiece (3, 4, 5)

Fig. 8. The additional sources of AE signal

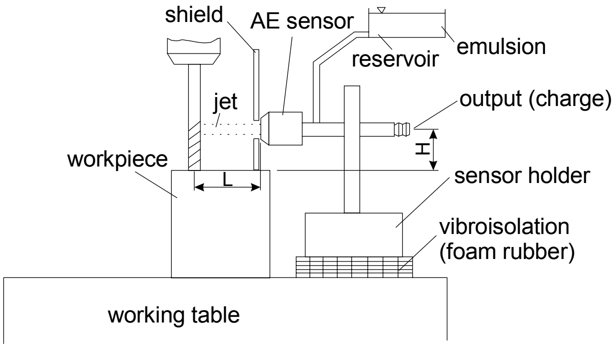

Fig. 9. AE signal acquisition with a fluidic sensor

d) Cutting conditions:
- rotational speed: 560 rev./min,
- feed rate: 0.12/rev.,
- flank wear VB = 0 mm (+0.03 mm).

e) Cutting conditions:
- rotational speed: 560 rev./min,
- feed rate: 0.12/rev.,
- flank wear VB = 0.15 mm (+0.03 mm).

f) Cutting conditions:
- rotational speed: 560 rev./min,
- feed rate: 0.12/rev.,
- flank wear VB = 0.37 mm (+0.03 mm).

The values of $\overline{A}$ are shown in Figure 10. Table 1 shows relevant and significant differences between two $\overline{A}$'s. The Gaussian distribution of individual quantities of A was assumed, and t- and F-tests were used in these comparisons (at a level of significance 0.05). Increase in rotational speed and/or feed rate resulted in an increase of $\overline{A}$. The increase in tool wear resulted in a decrease of intensity of AE signal, therefore $\overline{A}$ at VB=0.15 mm was significantly lower than $\overline{A}$ at VB=0 mm. In addition, $\overline{A}$ at VB=0.37 was significantly lower than $\overline{A}$ at VB=0.15 mm.

From the experiments with the fluidic AE sensor one can conclude:
1. In frequency range of interest (180 - 220 kHz) the intensity of AE signal decreased if the tool wear increased.
2. Rotational speed and feed rate significantly influenced the AE signal. The relation between these two parameters on the one hand and intensity of AE signal on the other hand is approximately proportional.
3. Rotational speed and feed rate had significant influence on the AE signal which hazed the cutting process monitoring.
4. Under given circumstances the tool wear can be predicted out of the AE signal. This prediction is successful only if the rotational speed and feed rate are constant.

Table 1

Comparisons of $\overline{A}$ (D: significant difference)

	a)	b)	c)	d)	e)	f)
a)	/	/	/	/	/	/
b)	D	/	/	/	/	/
c)	D		/	/	/	/
d)	D			/	/	/
e)				D	/	/
f)					D	/

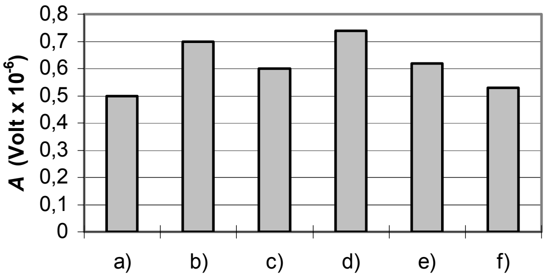

Fig. 10. $\overline{A}$ for various cutting conditions

The comparison of the experimentation with the contact and fluidic AE sensor (drilling in C15E steel) shows that in both cases the energy of AE signal decreases if the tool wear increases. This indicates that under the given circumstances rather the cutting process (or the tool wear) itself than the measuring method significantly influences the AE signal.

4. Conclusions

The measured AE data are relative, which suggest the development of an expert-based system and a database for AE signal acquisition and analysis [14,15].

For both tested materials the changes in the distance between the sensor and borehole did not significantly influence the AE signal. However, for both C15E steel and GG40 nodular gray iron the drill wear had a significant influence on the AE signal. In the analyzed frequency range the increase in tool wear resulted (i) in decrease of AE energy for steel and (ii) in increase of AE energy for gray iron. At VB=0.02 mm the energy of AE signal was higher when drilling into steel but at VB=0.12 mm the energy was equal for both materials. This cannot be explained only with graphite nodules in gray iron which presumably result in higher energy losses of AE signal in comparison to steel. For a thorough analysis of this matter, the influence of chip formation and friction between the tool and the workpiece should also be considered [16,17].

It is evident that for the selected cutting parameters and for both C15E steel and GG40 gray iron the monitoring of the drill wear is possible during the drilling process. Based on the additional experimentation with the fluidic sensor it is reasonable to conclude that under the given circumstances rather the tool wear than the measuring method influences the AE signal.

References

[1] G. Byrne, D. Dornfeld, I. Inasaki, G. Ketteler, W. König, R. Teti, Tool condition monitoring (TCM) - the status of research and industrial applications, Annals of the CIRP 44/2 (1995) 541-568.

[2] G.E. D'Errico, Adaptive systems for machining process monitoring and control, Journal of Materials Processing Technology 64 (1997) 75-84.

[3] S.Y. Liang, R.L. Hecker, R.G. Landers, Machining process monitoring and control: the state-of-the-art, Journal of Manufacturing Science and Engineering 126 (2004) 297-310.

[4] J. Kopac, Influence of cutting material and coating on tool quality and tool life, Journal of Materials Processing Technology 78 (1998) 95-103.

[5] M. Sokovic, J. Kopac, L.A. Dobrzanski, M. Adamiak, Wear of PVD-coated solid carbide end mills in dry high-speed cutting, Journal of Materials Processing Technology 157-158 (2004) 422-426.

[6] J. Kopac, The influence of Cr on tool wear by machining, Journal of Materials Processing Technology 157-158 (2004) 354-359

[7] S. Dolinsek, M. Brezocnik, J. Kopac, Mechanism and types of tool wear; some particularties in using advanced cutting materials and newest machining processes, Proceedings of the Scientific International Conference Achievements in Mechanical and Materials Engineering AMME'99, 1999, 58-63.

[8] I. Inasaki, Application of acoustic emission sensor for monitoring machining processes, Ultrasonics 36 (1998) 273-281.

[9] H.K. Toenshoff, M. Jung, S. Maennel, W. Rietz, Using acoustic emission signals for monitoring of production processes, Ultrasonics 37 (2000) 681-686.

[10] D.E. Lee, I. Hwang, C.M.O. Valente, J.F.G. Oliveira, D.A. Dornfeld, Precision manufacturing process monitoring with acoustic emission, International Journal of Machine Tools and Manufacture, 46/2 (2006) 176-188.

[11] C.E. Everson, S. H. Cheraghi, The application of acoustic emission for precision drilling process monitoring, International Journal of Machine Tools and Manufacture, 39/3 (1999) 371-387.

[12] J. Jurkovic, S. Sali, Indentification of dynamical behaviour by machining process, Journal of Mechanical Engineering, 48/3 (2002) 143-157.

[13] S. Sali, J. Kopac, Machining technology and experimental methods. Faculty of Mechanical Engineering, Ljubljana, Slovenia, 2003.

[14] A. Paszek, R. Knosala, The method of the knowledge representation in an expert system for metal cutting engineering, Journal of Materials Processing Technology 64 (1997) 319-326.

[15] B. Mursec F. Cus, Integral model of selection of optimal cutting conditions from different databases of tool makers, Journal of Materials Processing Technology 133 (2003) 158-165.

[16] S. Dolinsek, Work-hardening in the drilling of austenitic stainless steels, Journal of Materials Processing Technology 133 (2003) 63-70.

[17] S. Dolinsek, S. Ekinovic, J. Kopac, A contribution to the understanding of chip formation mechanism in high-speed cutting of hardened steel, Journal of Materials Processing Technology 157-158 (2004) 485-490.